AD-A069 156 ARMY ARMAMENT RESEARCH AND DEVELOPMENT COMMAND ABERD--ETC F/G 7/4
THE H+O2 YIELDS OH+O REACTION, A COMPARISON OF POTENTIAL SURFAC--ETC(U)
MAR 79 A GAUSS

UNCLASSIFIED ARBRL-TR-02148 SBIE-AD-E430 221 NL

| OF |
AD
A069156

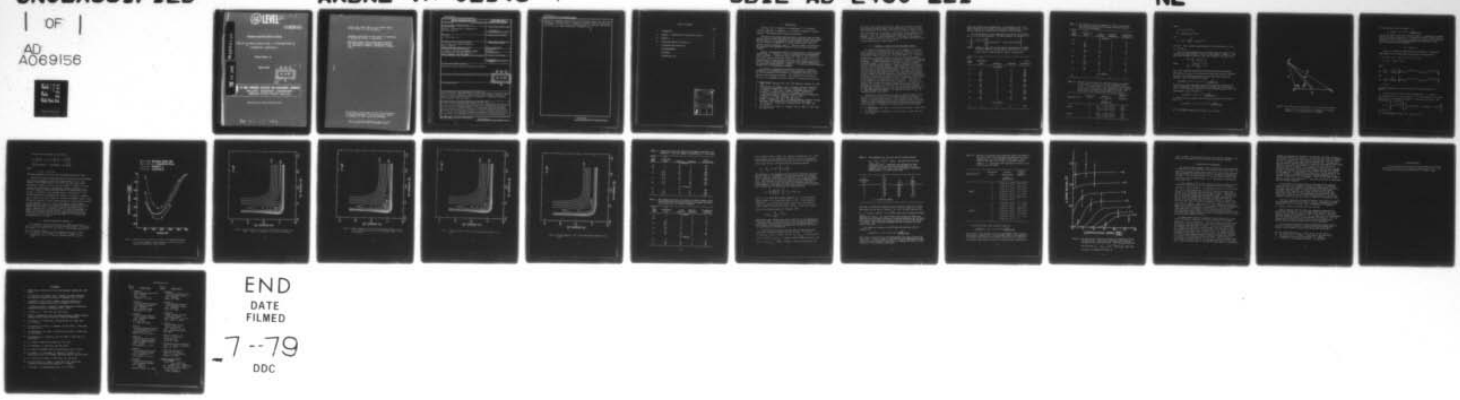

END
DATE
FILMED
7-79
DDC

(12) LEVEL III
B.S.

AD-E430 221

AD A069156

DDC FILE COPY

TECHNICAL REPORT ARBRL-TR-02148

THE $H+O_2 \rightarrow OH+O$ REACTION, A COMPARISON OF POTENTIAL SURFACES

Arthur Gauss, Jr.

March 1979

DDC
RECEIVED
MAY 30 1979
B

US ARMY ARMAMENT RESEARCH AND DEVELOPMENT COMMAND
BALLISTIC RESEARCH LABORATORY
ABERDEEN PROVING GROUND, MARYLAND

Approved for public release; distribution unlimited.

79 04 26 400

Destroy this report when it is no longer needed.
Do not return it to the originator.

Secondary distribution of this report by originating or sponsoring activity is prohibited.

Additional copies of this report may be obtained from the National Technical Information Service, U.S. Department of Commerce, Springfield, Virginia 22161.

The findings in this report are not to be construed as an official Department of the Army position, unless so designated by other authorized documents.

The use of trade names or manufacturers' names in this report does not constitute indorsement of any commercial product.

UNCLASSIFIED

SECURITY CLASSIFICATION OF THIS PAGE (When Data Entered)

REPORT DOCUMENTATION PAGE	READ INSTRUCTIONS BEFORE COMPLETING FORM
1. REPORT NUMBER: Technical Report ARBRL-TR-02148 / 2. GOVT ACCESSION NO.	3. RECIPIENT'S CATALOG NUMBER
4. TITLE (and Subtitle): The $H+O_2 \rightarrow OH+O$ Reaction, A Comparison of Potential Surfaces	5. TYPE OF REPORT & PERIOD COVERED: BRL Report
	6. PERFORMING ORG. REPORT NUMBER
7. AUTHOR(s): Dr. Arthur Gauss, Jr.	8. CONTRACT OR GRANT NUMBER(s)
9. PERFORMING ORGANIZATION NAME AND ADDRESS: US Army Ballistic Research Laboratory, ATTN: DRDAR-BLB, Aberdeen Proving Ground, MD 21005	10. PROGRAM ELEMENT, PROJECT, TASK AREA & WORK UNIT NUMBERS: RDT&E 1L161102AH43
11. CONTROLLING OFFICE NAME AND ADDRESS: US Armament Research & Development Command, US Army Ballistic Research Laboratory, ATTN: DRDAR-BL, APG, MD 21005	12. REPORT DATE: MARCH 1979
	13. NUMBER OF PAGES: 27
14. MONITORING AGENCY NAME & ADDRESS (if different from Controlling Office)	15. SECURITY CLASS. (of this report): Unclassified
	15a. DECLASSIFICATION/DOWNGRADING SCHEDULE

16. DISTRIBUTION STATEMENT (of this Report)

Approved for public release; distribution unlimited.

DDC
RECEIVED
MAY 30 1979
B

17. DISTRIBUTION STATEMENT (of the abstract entered in Block 20, if different from Report)

18. SUPPLEMENTARY NOTES

19. KEY WORDS (Continue on reverse side if necessary and identify by block number)

Chemical reactions, $H+O_2 \rightarrow OH+O$ reaction, chemical trajectory calculations, Monte Carlo trajectory calculations, LEPS potential energy surfaces, comparison of potential energy surfaces, vibrational enhancement of endothermic reactions, Sato parameters, Morse potentials.

20. ABSTRACT (Continue on reverse side if necessary and identify by block number) (hmn)

A new two Sato parameter LEPS surface has been developed for the $HO_2^{\ddagger}$ system. The force constants and equilibrium geometry are in better accord with experiment than the corresponding properties of the previous single Sato parameter surfaces (Surfaces I and I'). Trajectory calculations have been run using the new surface for the $H+O_2^{\ddagger}$ reaction with $O_2^{\ddagger}$ in initial vibrational states v=0,3,4 and 6. Results still indicate vibrational enhancement of the reaction rate but the magnitude of the enhancement is much less than for the previous surfaces.

(over)

DD FORM 1 JAN 73 1473 EDITION OF 1 NOV 65 IS OBSOLETE

UNCLASSIFIED

SECURITY CLASSIFICATION OF THIS PAGE (When Data Entered)

79 04 26 400

Specific rate constants are calculated and the overall thermal rate constant is estimated at 1600°K and 2500°K. In addition a difficulty with the single parameter Surface I has been corrected yielding Surface I'. Specific rates and an overall rate are estimated using those surfaces as well.

TABLE OF CONTENTS

ACCESSION for
NTIS White Section ☑
DDC Buff Section ☐
UNANNOUNCED ☐
JUSTIFICATION
BY
DISTRIBUTION/AVAILABILITY CODES
Dist. AVAIL. and/or SPECIAL
A

I. INTRODUCTION

The $H+O_2 \rightarrow OH + O$ reaction is an endothermic ($\sim$ 17 kcal/mole) reaction[1] important in combustion. It continues to appear in reaction schemes[2-4] describing various combustion processes.

Trajectory calculations have been used to calculate cross sections, specific rate constants and estimates of the overall thermal rate constant for the reaction. A new potential surface (Surface II) has been used which fits the known properties of the HO_2 complex better than two previous surfaces (Surfaces I and I′). The new surface is described by two adjustable Sato parameters instead of one as in the two previous surfaces.

Surface I and associated results were discussed in a previous paper[5] (called Paper I). Surface I′ corrects a problem which was subsequently found in Surface I. Trajectory results for Surface I′ are reported in this report along with those for Surface II. The classical trajectory program CLASTR[6], suitably modified for these LEPS surfaces, was used for all the trajectory calculations. Surface I′ shows little difference in the trajectory results relative to Surface I. It also has similar potential contours for all configurations compared.

The results of trajectory calculations on Surface II indicate enhancement of the reaction rate due to vibrational excitation of the O_2, but the magnitude of this effect is considerably less than on the previous single parameter surfaces. This vibrational enhancement of the rate is in agreement with other studies[7,8] on endothermic reactions.

1. JANAF Tables, edited by D.R. Stull (Dow Chemical, Midland, MI, 1965-1967).
2. M.B. Collset, D.W. Naegeli, and I. Glassman, Sixteenth Symposium on Combustion (Combustion Institute, Pittsburgh, 1977) p. 1023.
3. T. Miyauchi, Y. Mori, and A. Imamura, Sixteenth Symposium on Combustion, (Combustion Institute, Pittsburgh, 1977) p.1073.
4. G. Dixon-Lewis and R.J. Simpson, Sixteenth Symposium on Combustion, (Combustion Institute, Pittsburgh, 1977) p. 1111.
5. A. Gauss, Jr., J. Chem. Phys. 68, 1689 (1978).
6. CLASTR is program No. 229 in the Quantum Chemistry Program Exchange Catalogue (QCPE, Indiana University, Chemistry Department).
7. D.S. Perry, J.C. Polanyi and C. Woodrow Wilson, Jr., Chem. Phys. 3, 317 (1974).
8. R.N. Porter, L.B. Sims, D.L. Thompson, and L.M. Raff, J. Chem. Phys. 58, 2855 (1973).

The results show clearly that the most significant changes in specific reaction rates between Surface II and Surfaces I and I′ occur for the lower vibrational states (v=0,1,2) of the O_2 whereas the higher states (v=3,4,5,6) show less of an effect. Surface II is quite different from Surfaces I and I′ in the high interaction region (all nuclei close together). That even small differences in the shape of the potential in this region can affect the reactivity in the lowest vibrational level has been demonstrated by other workers[9,10].

II. SURFACE I′, DESCRIPTION AND TRAJECTORY RESULTS

The trajectory results for Surface I′ are summarized in Tables I and II, similar to the presentation of results in Paper I. As in that study trajectories are run in sets for which the sum of the relative translational energy (E_R) plus the vibrational energy (E_v) is constant. The majority of trajectory points were run with rotational quantum number J=1 (corresponding to about a hundreth of a kcal/mole of rotational energy). A number of points were run with J=21 (about 2 kcal/mole of rotational energy). Three types of trajectory events are defined: reactive, nonreactive, and complex. Complex trajectories are long trajectories that the CLASTR integrator cannot follow; they are not back integrable (energy and angular momentum are conserved). Both reactive and non-reactive events are back integrable. The complex trajectories have been further subdivided (Table II) into reactive complex and nonreactive complex trajectories according to the decision of the CLASTR integrator. Observe that in addition to some points for checking Surface I′ results against those of Surface I (Paper I) additional points were run on Surface I′ for vibrational levels v=3,2 and 1. They fill in nicely between the v=4 and v=0 results of Surface I. (See Paper I.) Specific rate constants have been evaluated for the v=3,2 and 1 levels assuming, as in Paper I, a constant average cross section over all translational energies down, of course, to the classical threshold. The maximum impact parameter used for the cross section calculations was 3 Å. These specific rate constants are tabulated in Table III for two temperatures, 1600°K and 2500°K.

The difficulty with Surface I was that it had an infinity in the derivatives of the potential in the linear configuration (θ=180°). Surface I′ eliminates this infinity. This infinity causes little difference in the trajectories results between Surfaces I and I′ since the system very rarely approaches the linear or near linear configuration even on Surface I′. Because of the large potential hole the system

9. N. Sathyamurthy, J.W. Duff, C. Stroud, and L.M. Raff, J. Chem. Phys. 67, 3563 (1977).
10. N. Sathyamurthy, R. Rangarajan, and L.M. Raff, J. Chem. Phys. 64, 4606 (1976).

definitely prefers bent configurations. Also Surfaces I and I′ are nearly identical in well depth and equilibrium configuration. The potential contours are similar for all values of the H-0-0 angle.

The only difference in the mathematical form of the two surfaces I and I′ is in the Sato parameter. The Sato parameter for Surface I′ is

$$\Delta' = \left\{ 1-e^{-\left(x_{a/b}\right)^2} \right\} \left\{ 0.53(\sin 2Th)^2 - 0.25(\cos Th)^2 + 0.2\left(\frac{\pi}{2}\right)^2 \right\}$$

TABLE I. Summary of the reactive and complex trajectories for Surface′. The total number of trajectories for each initial 0_2 vibrational level in each energy set (E_R+E_v) are given also.

E_R+E_v kcal/mole	0_2 Vibrational Level	Reactions	Complexes	Total Trajectories
		J=1 RESULTS		
33	6	16	16	300
29	3	1	6	500
	2	1	0	500
	1	0	0	500
24	4	7	24	300
	3	4	15	500
22	2	1	10	500
	1	0	1	500
18	3	1	72	500
	2	0	18	500
	1	1	3	500
14	2	0	44	500
	1	0	18	500
		J=21 RESULTS		
33	6	15	12	300

TABLE II. The complex trajectories tabulated in Table I are divided into reactive and non reactive groups using the decision of the CLASTR integrator.

E_R+E_V kcal/mole	O_2 Vibrational Level	Total Complexes	Reactive Complexes	Non-Reactive Complexes
		J=1 RESULTS		
33	6	16	4	12
29	3	6	1	5
	2	0	0	0
	1	0	0	0
24	4	24	5	19
	3	15	2	13
22	2	10	1	9
	1	1	0	1
18	3	72	5	67
	2	18	1	17
	1	3	0	3
14	2	44	0	44
	1	18	0	18
		J=21 RESULTS		
33	6	12	4	8

TABLE III. Specific rate constants (at 1600°K and 2500°K) for Surface I′ are given for O_2 initially in the vibrational levels v=3,2,1. The populations of the vibrational levels relative to the v=0 level are shown. All calculations were done with an initial O_2 rotational quantum number (J) of one. The errors quoted are the Monte Carlo statistical errors.

Temperature (°K)	Vibrational Level	Specific Rate Constant $\frac{cm^3}{molecule\ sec}$	Relative Level Population
1600°K	3	$(6.7 \pm 4.4) \times 10^{-12}$	.016
	2	$(1.3 \pm 1.3) \times 10^{-12}$	.063
	1	$(0.29 \pm 0.29) \times 10^{-12}$	.246
2500°K	3	$(8.3 \pm 5.5) \times 10^{-12}$	.073
	2	$(1.9 \pm 1.9) \times 10^{-12}$	.171
	1	$(0.61 \pm 0.61) \times 10^{-12}$	.410

where

$$b = 0.6 \times 10^{-8} \text{ cm.}$$

$$Th = \text{Arcsin}(r_1/x_a \sin\theta)$$

and

$$x_a = (r_1^2 + r_2^2/4 - r_1 r_2 \cos\theta)^{1/2} \quad .$$

See Fig. 1 for a pictorial representation of the parameters x_a, Th, θ, r_1, r_2, and r_3.

The total rate constant may be evaluated using the specific rate constant data from Surface I′ (Table III) and Surface I (Paper I). The total rate constant is given by (only odd J appear in the sum for O_2)

$$K(T) = \sum_{v,J} F_{BC}(v,J)\, k_{vJ}$$

where

$$F_{BC} = \frac{f_J(2J+1)e^{-E_{v,J}/kT}}{Q_{Jv}}$$

F_{BC} is the rotational-vibrational distribution function (Boltzmann distribution) and Q_{Jv} is the rotational-vibrational partition function. The total rate constant evaluated from the trajectory results for Surfaces I and I′ at 1600°K is given by

$$K_T(1600°K) = (3.0 \pm 2.0) \times 10^{-13} \ \frac{cm^3}{\text{molecule sec}} \quad .$$

This value has been evaluated neglecting the possible contribution of reactive complexes. The error quoted is the Monte Carlo statistical error. The contribution from the v=0 level has been taken as zero. The experimental value of Schott[11] is

$$K_E(1600°K) = 1.35 \times 10^{-12} \ \frac{cm^3}{\text{molecule sec.}} \quad .$$

At 2500°K the rate constant from the trajectory results of Surfaces I and I′ is

$$K_T(2500°K) = (1.7 \pm 0.9) \times 10^{-12} \ \frac{cm^3}{\text{molecule sec.}} \quad .$$

11. G.L. Schott, Combustion and Flame, 21, 357 (1973).

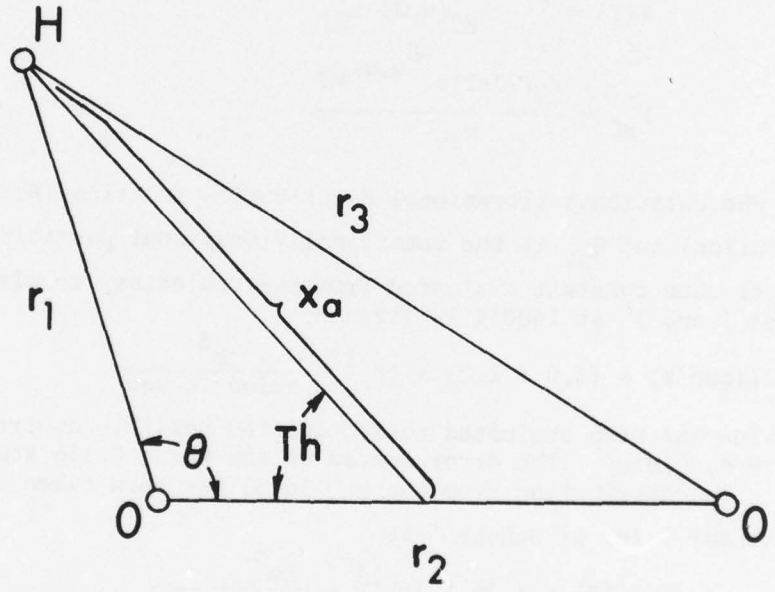

Figure 1. The internuclear coordinates r_1, r_2, and r_3 and the H-O-O angle (θ) are defined as shown. The angle "Th" and the distance "x_a" are displayed on the diagram.

The experimental result of Schott[11] is

$$K_E(2500°K) = 5.9 \times 10^{-12} \frac{cm^3}{\text{molecule sec.}} .$$

As with the 1600°K result the trajectory result is a minimum rate constant (neglecting reactive complexes). If the decision of the CLASTR integrator in regard to the reactivity of the complexes is assumed correct, then both trajectory results would be doubled, bringing the trajectory results within a factor of two of experiment.

III. SURFACE II

Surface II contains two adjustable Sato parameters. The general LEPS potential for a three atom system has the following form[12]

$$V = Q_1' + Q_2' + Q_3' - (\alpha_1'^2 + \alpha_2'^2 + \alpha_3'^2 - \alpha_1'\alpha_2' - \alpha_1'\alpha_3' - \alpha_2'\alpha_3')^{\frac{1}{2}} + D_2^e$$

where

$$Q_i' = \frac{Q_i}{1+\Delta_i} = \frac{D_i^e}{4(1+\Delta_i)} \left\{ \left(3+\Delta_i\right) e^{-2\beta_i(r_i-r_{io})} - \left(2+6\Delta_i\right) e^{-\beta_i(r_i-r_{io})} \right\}$$

and

$$\alpha_i' = \frac{\alpha_i}{1+\Delta_i} = \frac{D_i^e}{4(1+\Delta_i)} \left\{ \left(1+3\Delta_i\right) e^{-2\beta_i(r_i-r_{io})} - \left(6+2\Delta_i\right) e^{-\beta_i(r_i-r_{io})} \right\}$$

$i = 1,2,3.$

The Morse parameters for the two diatomics OH and O_2 are given in Paper I.

In the present case the two Sato parameters are: 1) $\Delta=\Delta_1=\Delta_3$ (OH parameter) and 2) Δ_2 (O_2 parameter). The Sato parameter Δ is closely similar to the Δ' defined for Surface I′ in the previous section. The Sato parameter Δ is given by

$$\Delta = 0.7 \left\{ 1-e^{-\left(x_{a/b}\right)^2} \right\} \left\{ 0.53(\sin 2Th)^2 - 0.25(\cos Th)^2 + 0.2(\pi/2)^2 \right\}$$

(see Fig. 1).

12. J.T. Muckerman, J. Chem. Phys. 56, 2997 (1972).

The other Sato parameter Δ_2 is given by

$$\Delta_2 = \left\{ \sin(c \cdot r_2) + .15 \cdot \left[\sin(c \cdot r_2) \right]^8 \right\}$$

$$* \left\{ 0.53(\sin 2Th)^2 - 0.25(\cos Th)^2 + 0.2 \left(\frac{\pi}{2}\right)^2 \right\}$$

where

$$c = \pi/5.2 \times 10^{-8} \text{ cm.}$$

The other parameters, Th and r_2 have been defined previously (Fig. 1).

Surface II yields an equilibrium position for HO_2 in better agreement with recent experimental results than either Surface I or I′. For Surface II the minimum energy is at r_1=0.99, r_2=1.30, θ=105° versus experimental values of r_1=0.985, r_2=1.36, θ=106°.[13] Surface II is also a better fit to the shape of the potential minimum than either I or I′. The force constants reported from the analysis of experimental results are f_{OH} = 6.5 mdyne/Å, f_{OO}=5.8 mdyne/Å and f_θ= 1.088 mdyne/Å.[14] The values from the new two parameter LEPS Surface II are f_{OH}= 6.1 mdyne/Å, f_{OO}=5.1 mdyne/Å, and f_θ=0.65 mdyne/Å. The new two parameter surface, like the previous surfaces, fits the angular variation of the potential as given by Gole and Hayes (Fig. 2)[15]. For $\theta \leq 95°$ there is some divergence between Surface II and the CI results; the LEPS fitting function is not sufficiently flexible to closely follow the ab initio data in this region. However, the CI calculation itself is very limited, using only minimal basis set SCF generated orbitals. The differences between Surface II and Surface I can be seen by comparing the potential plots for Surface II at θ=80,108,140, and 180° (Figs. 3, 4, 5, 6) with the corresponding plots in Paper I.

IV. TRAJECTORY RESULTS FOR SURFACE II.

The trajectory results for Surface II are summarized in Tables IV and V. The mode of presentation is similar to that in Paper I and to that for Surface I′ in Section II of this article. Trajectories were run for

13. J.F. Ogilvie, Canadian Journal of Spectroscopy, 19, 171 (1973).
14. S. Farantos, E.C. Leisegang, J.N. Murrell, K. Sorbie, J.J.C. Texeira-Dias, and A.J.C. Verandas, Molecular Physics, 34, 947 (1977).

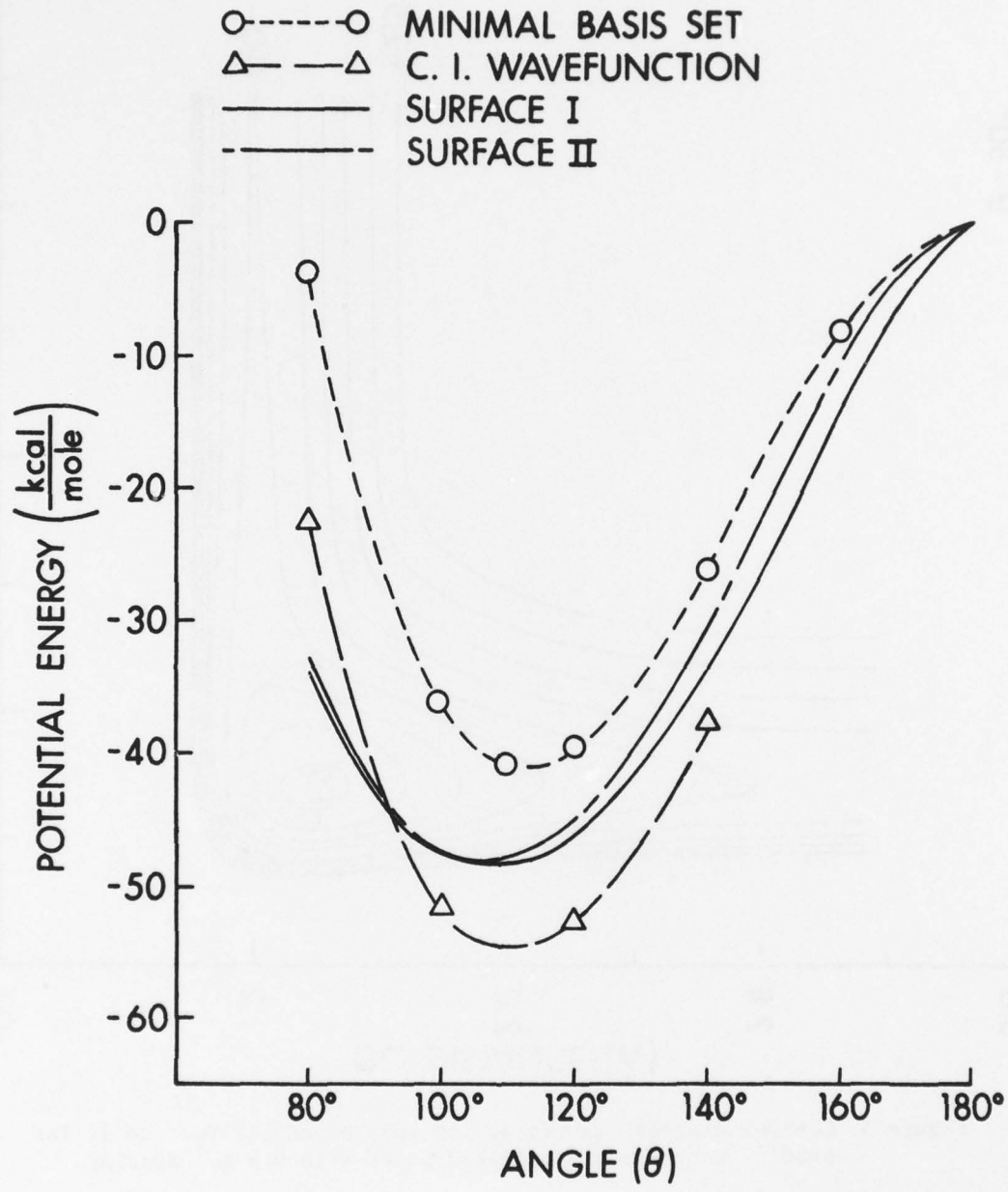

Figure 2. Comparison (at r_1=0.96Å, r_2=1.23Å) of the angular dependence of the LEPS potential energy Surface II with the ab initio surfaces calculated by Gole and Hayes.

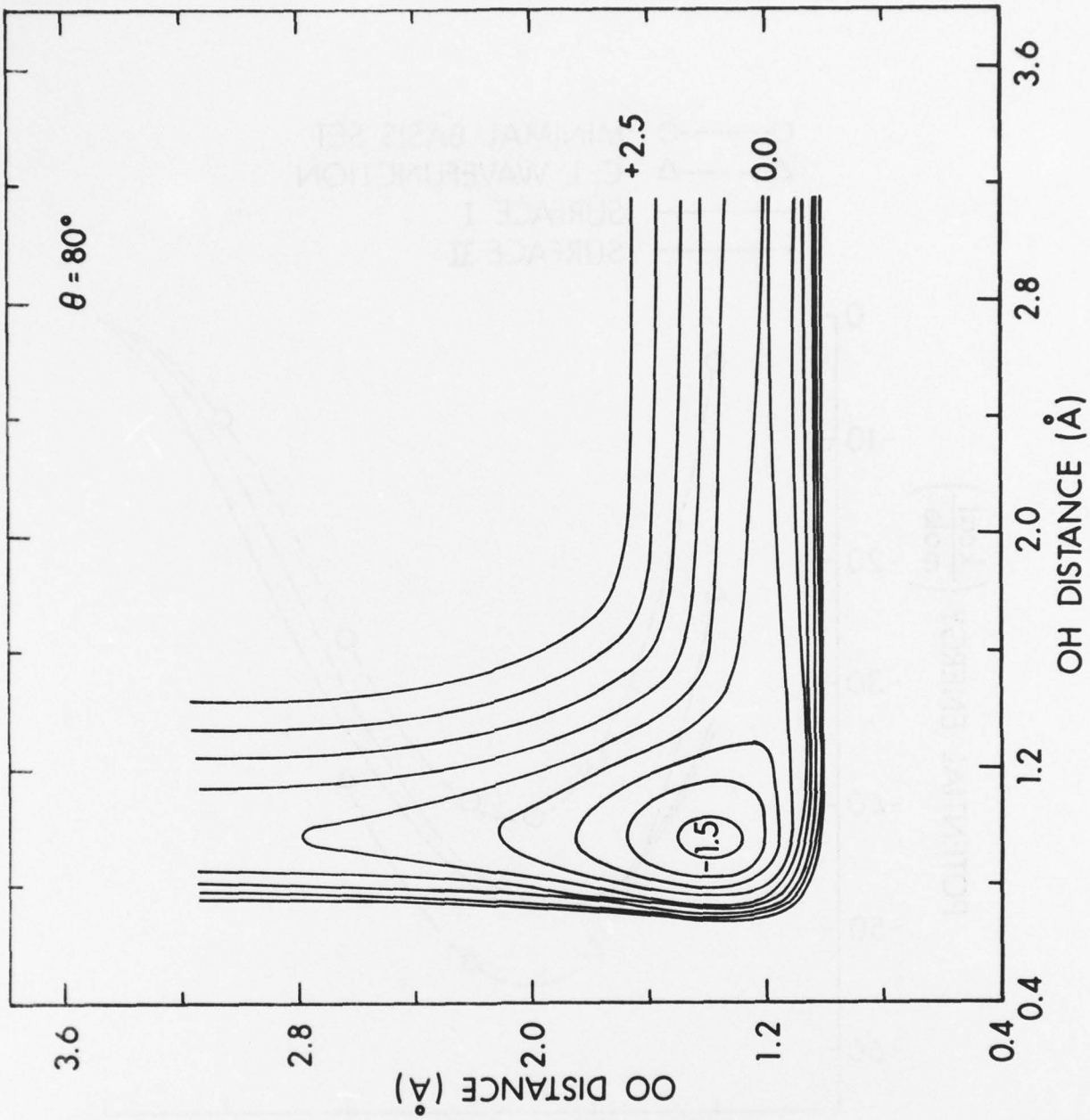

Figure 3. Contour diagram (in eV) of the LEPS potential Surface II for $\theta=80°$. Contours are labelled in eV with 0.5 eV. spacing.

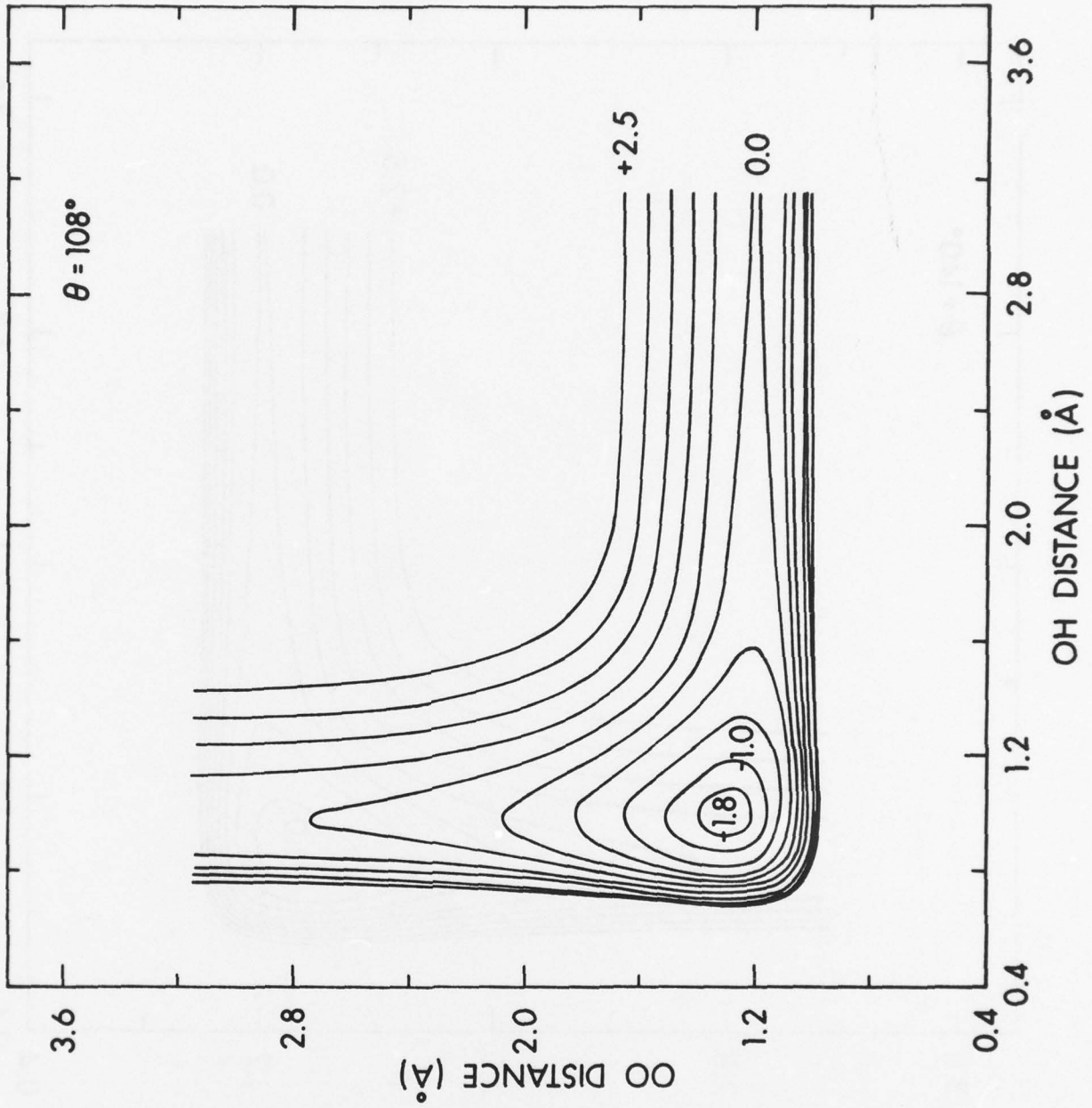

Figure 4. Contour diagram (in eV) of the LEPS potential Surface II for $\theta=108°$; the potential well is near its greatest depth (~2 eV.) at this angle.

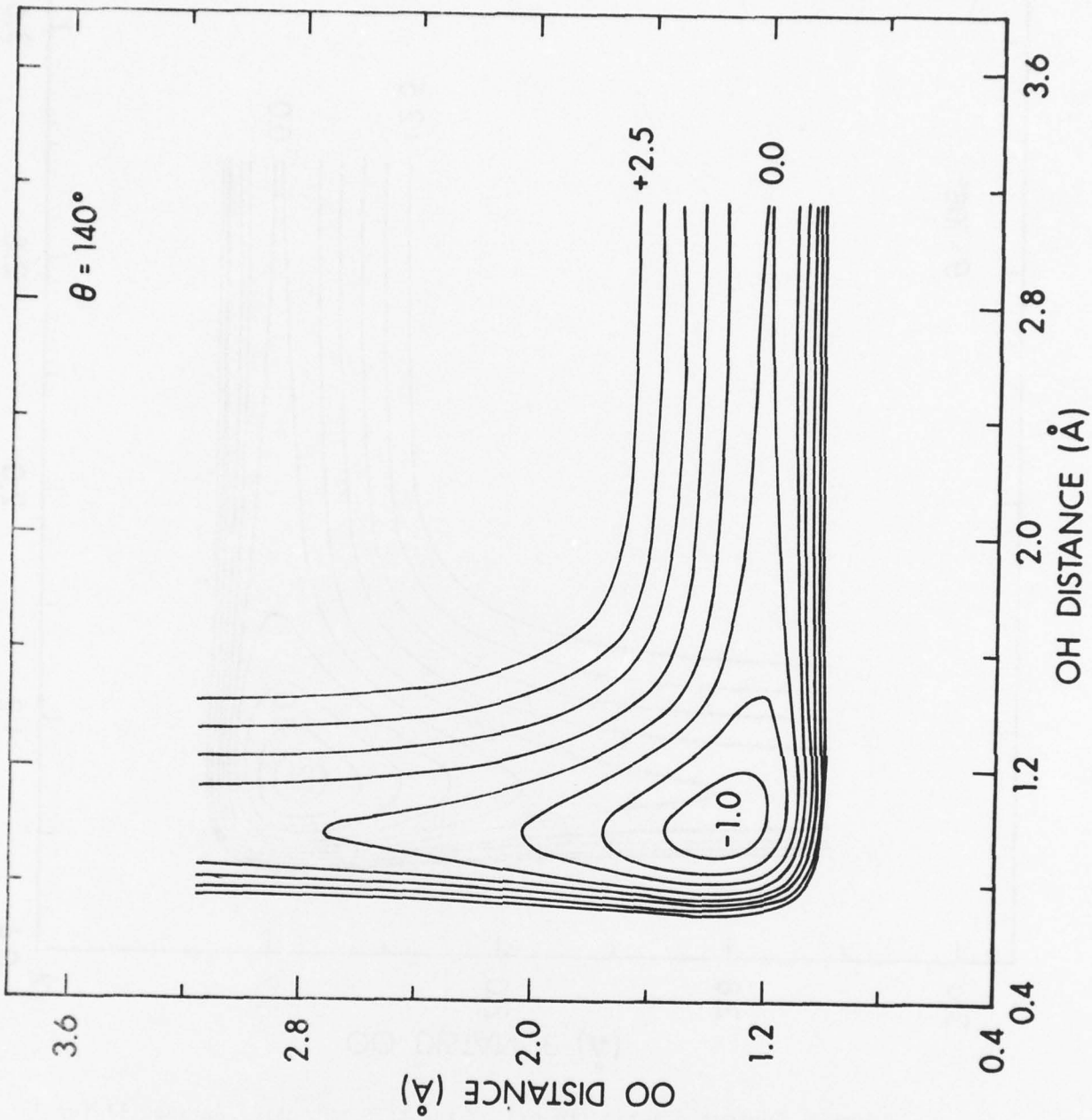

Figure 5. Contour diagram (in eV) of the LEPS potential Surface II for $\theta=140°$.

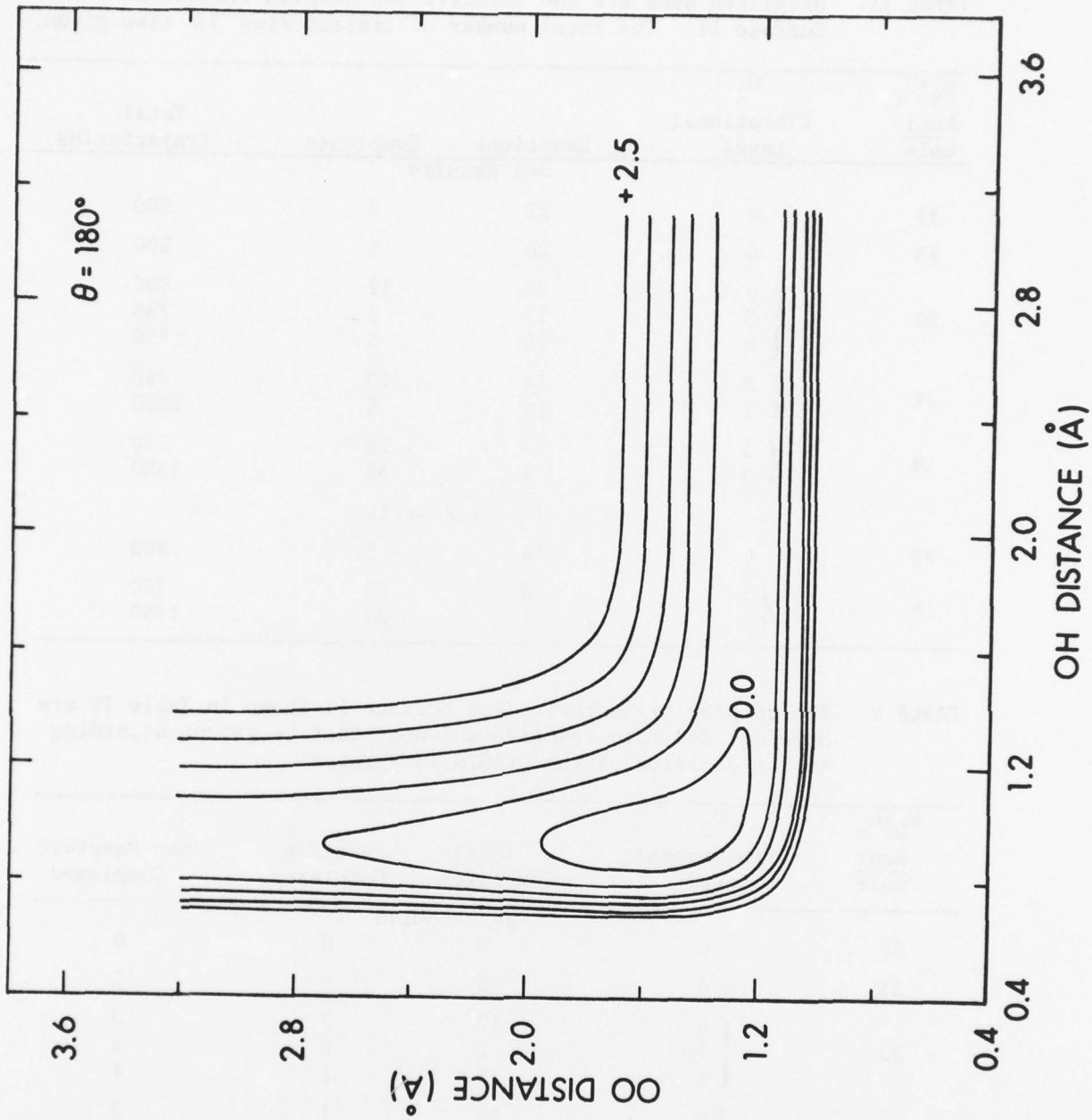

Figure 6. Contour diagram (in eV) of the LEPS potential Surface II for θ=180°.

TABLE IV. Displayed here are the reactive and complex trajectories for Surface II. The total number of trajectories is also given.

E_R+E_v kcal/mole	O_2 Vibrational Level	Reactions	Complexes	Total Trajectories
		J=1 Results		
38	6	22	0	500
33	6	26	5	500
29	6	22	12	500
	3	17	2	750
	0	10	5	1350
24	3	14	10	750
	0	16	5	1350
18	3	3	26	750
	0	4	30	1350
		J = 21 Results		
33	6	34	5	500
18	3	8	30	750
	0	7	24	1350

TABLE V. The complex trajectories for Surface II shown in Table IV are here divided into reactive and non-reactive groups according to the decision of the CLASTR integrator.

E_R+E_v kcal/mole	O_2 Vibrational Level	Total Complexes	Reactive Complexes	Non-Reactive Complexes
		J=1 RESULTS		
38	6	0	0	0
33	6	5	0	5
29	6	12	2	10
	3	2	0	2
	0	5	1	4
24	3	10	1	9
	0	5	0	5
18	3	26	1	25
	0	30	3	27
		J-21 RESULTS		
33	6	5	0	5
18	3	30	2	28
	0	24	2	22

three different values of E_R+E_V (E_R, relative translational, + E_V, vibrational energy) for each vibrational level v=0, 3 and 6. Trajectories were run for one value of $E_R + E_V$ for the v=4 level. The minimum cross section data of Fig. 7 are fitted with the following function

$$S_{r_{vJ}} = S^{o}_{r_{vJ}} + \frac{1}{\kappa} \tan^{-1} \left\{ \lambda (E-E_o) \right\} \quad .$$

The constants in this expression for the various vibrational levels are shown in Table VI. Interpolation was used to determine the constants for the levels for which there is no data (v=1,2,5) or only one datum (v=4). Note that the v=4 trajectory point fits the interpolated curve well. The thresholds for each cross section function of the three lowest levels (v=0,1,2) are a few tenths of a kcal/mole below the classical thresholds. From these analytical cross section curves the specific rate constants may be derived using the usual expression

$$k_{vJ} = \left\{ \frac{8kT}{\pi \mu_{A,BC}} \right\}^{\frac{1}{2}} \int_o^{\infty} S_{r_{vJ}} f(T,E_R)\, dE_R$$

where v is the vibrational quantum number of O_2, J is the rotational quantum number of O_2 (always odd either 1 or 21), T is the absolute temperature, $\mu_{A,BC}$ is the reduced mass of H,O_2, E_R is the collision energy (relative translational energy), and $S_{r_{vJ}}$ is the cross section given by the function previously described. Also

$$f(T,E_R) = \frac{E_R}{(kT)^2} \, e^{-E_R/kT} \quad .$$

The specific rate constants are shown in Table VII at two temperatures, 1600°K and 2500°K. If rotational effects can be neglected and assuming a Boltzmann distribution of vibrational energy, the overall thermal rate constant can be estimated (assuming also vibrational levels above v=6 make negligible contributions).

In the case of the v=6 and v=0 states the J=21 data do not show statistically greater reactivity than the J=1 data. For the v=6, J=1 state $S_{r_{6,1}} = (1.47 \pm 0.28)\text{Å}^2$, for v=6, J=21, $S_{r_{6,21}} = (1.92 \pm 0.32)\text{Å}^2$, for the v=0, J=1 state $S_{r_{0,1}} = (.0838 \pm 0.0418)\text{Å}^2$, and for the v=0, J=21 state we have $S_{r_{0,21}} = (.1466 \pm 0.0552)\text{Å}^2$. For the v=3 state the J=21

TABLE VI. The parameters for the cross section fitting function

$$S_{r_{vJ}} = S^{o}_{r_{vJ}} + \frac{1}{\kappa} \tan^{-1} \lambda(E-E_o)$$ are given here for each vibrational level. Parameters were adjusted for cross sections fits to the v=0,3 and 6 levels data only, the parameters for other levels were interpolated. Rotational quantum number J is equal to one (J=1).

O_2 Vibrational Level	$S^{o}_{r_{vJ}}$ (J=1) ($Å^2$)	κ ($Å^{-2}$)	E_o $\frac{kcal}{mole}$
6	.60	122.5	-8.0
5	.49	150	-3.7
4	.388	189	0.7
3	.30	245	5.0
2	.228	322	9.4
1	.176	418	1.37
0	.15	490	18.0

λ = 1/2 FOR ALL LEVELS

data show statistically somewhat greater reactivity than the J=1 data. The results are for the J=1 state $S_{r_{3,1}} = (1.131 \pm 0.652)Å^2$ and for J=21, $S_{r_{3,21}} = (3.016 \pm 1.061)Å^2$. In all cases above the J=21 data are larger than the J=1 results. The total thermal rate constant at 1600°K and 2500°K will be calculated assuming no rotational dependence but the above data indicate that these total thermal rates may be 50 to 100% low due to rotation. This rotational dependence should be examined with more care in the future.

The total rate constant at 1600°K from the trajectory work on Surface II is

$$K_T(1600°K) = (1.45 \pm 0.49) \times 10^{-2} \frac{cm^3}{molecule\ sec.}$$

This result is quite close to the experimental value given earlier (see Section II). It must be kept in mind that reactive complexes have been neglected in this calculation and these will augment the result, as most likely will the rotational contribution.

TABLE VII - Specific rate constants (at 1600°K and 2500°K) for Surface II are given. These are derived from the cross section curves shown in Fig. 7. Errors are Monte Carlo errors. All calculations were done with initial O_2 rotational quantum number J = 1. Vibrational level populations relative to the v=0 level are also shown.

Temperature (°K)	Vibrational Level	Specific Rate Constant $\frac{cm^3}{molecule\ sec.}$	Relative Level Population
1600°K	6	$(7.4\pm1.5) \times 10^{-11}$	3.12×10^{-4}
	5	$(5.9\pm1.5) \times 10^{-11}$	1.13×10^{-3}
	4	$(4.1\pm1.2) \times 10^{-11}$	4.22×10^{-3}
	3	$(2.0\pm0.7) \times 10^{-11}$	1.6×10^{-2}
	2	$(6.4\pm2.2) \times 10^{-12}$	6.3×10^{-2}
	1	$(1.8\pm0.7) \times 10^{-12}$	2.46×10^{-1}
	0	$(5.1\pm1.8) \times 10^{-13}$	1
2500°K	6	$(9.4\pm1.9) \times 10^{-11}$	5.71×10^{-3}
	5	$(7.5\pm1.7) \times 10^{-11}$	1.3×10^{-2}
	4	$(5.5\pm1.4) \times 10^{-11}$	3.02×10^{-2}
	3	$(3.2\pm0.9) \times 10^{-11}$	7.27×10^{-2}
	2	$(1.5\pm0.5) \times 10^{-11}$	1.71×10^{-1}
	1	$(6.6\pm2.1) \times 10^{-12}$	4.1×10^{-1}
	0	$(3.0\pm1.0) \times 10^{-12}$	1

At 2500°K the total rate constant is given by

$$K_T(2500°K) = (7.9 \pm 2.4) \times 10^{-12} \frac{cm^3}{molecule\ sec.} .$$

This result is some 30% higher than the experimental result of Schott quoted earlier (Section II). The trajectory result is low because of the reasons stated above for $K_T(1600°K)$ and because of the neglect of vibrational levels above v=6 which will contribute more significantly

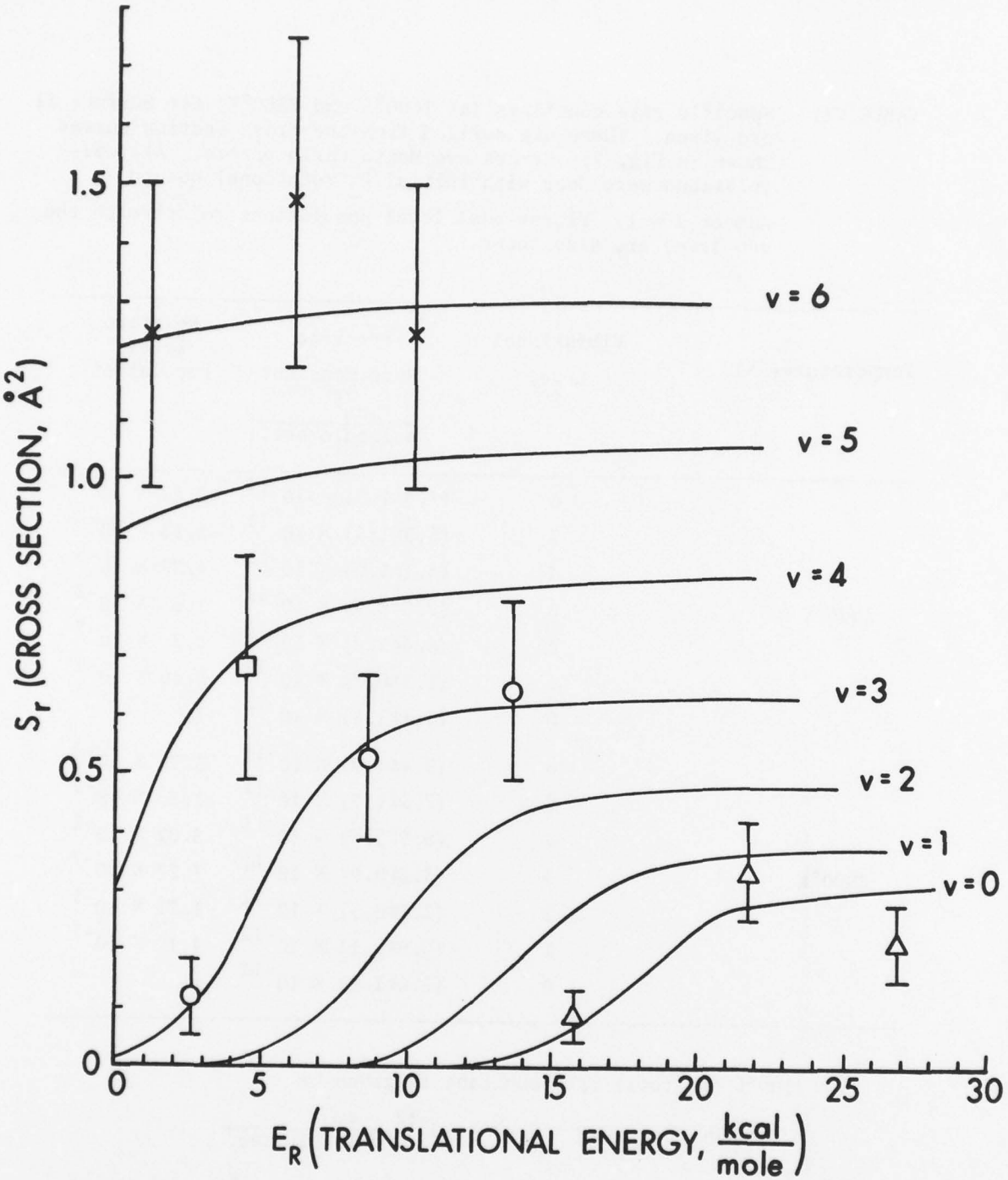

Figure 7. The minimum cross sections are shown as a function of translational energy. Monte Carlo statistical error bars are included at each trajectory point. The data are fitted with the functions $S_{r_{vJ}} = S^{o}_{r_{vJ}} + \frac{1}{\kappa} \tan^{-1} \left\{ \lambda(E-E_o) \right\}$ where the constants are displayed in Table VI.

than at 1600°K. The error result quoted with each rate constant is the Monte Carlo statistical error inherent in the trajectory method.

V. DISCUSSIONS AND CONCLUSIONS

By using two Sato parameters which are functions of the coordinates an improved LEPS surface (Surface II) for HO_2 has been constructed. The equilibrium geometry of this surface agrees more closely with experiment than the geometry of either Surface I or I′. However, the greatest improvement is in the force constants for the HO_2 complex which are much better than those of either Surface I or I′ and match the experimental values quite well.

As for Surfaces I and I′ the trajectory results for Surface II show significant enhancement in the $H+O_2$ reaction rate due to vibrational excitation of the O_2 molecule. An enhancement factor of ~ 150 at 1600°K and ~ 30 at 2500°K (between the v=0 and v=6 levels) is achieved for Surface II as indicated by the specific rate constants. These factors are not nearly so large as those for Surfaces I and I′. The reason they are not so large is clear from the specific reaction rate tables. At the v=6 level the specific rate constants (at 1600° and 2500°) for Surface II are very nearly equal to those for Surface I. However, as the vibrational level is decreased the Surface II specific rates do not drop nearly so rapidly. Other workers[9,10] have demonstrated that small changes in the inner reflective wall of potential surfaces can dramatically affect reactivity in the lowest vibrational level. The same sort of vibrational effect is noted here but the effect extends to levels above the lowest level. However, there are rather significant differences in the potential contours between Surface II and Surfaces I and I′ in the high interaction region in our case.

An added benefit of the new potential surface (Surface II) is the dramatic decrease in complexes formed for O_2 initially in the upper vibrational levels (v=3 and above). Thus the minimum cross sections and specific rate constants quoted for these levels are less uncertain due to complexes than those rates in Paper I. Even if all the complexes were assumed to be reactive (a worst possible case) then the specific rate constant for the v=3 level would be some two (at 2500°K) or three (at 1600°K) times larger than the minimum rates. If a more reasonable assumption is made, such as taking the decision of the CLASTR integrator as correct for the complex trajectories, then the minimum rate constant is only some 10% low (at both 1600°K and 2500°K). The v=6 level is considerably less uncertain than the v=3 level. Even for the worst case (all complexes reactive) for v=6, the minimum rate would be low by some 25% at 2500°K and 10% at 1600°K. For the v=0 level there is a significant

increase in complexes for Surface II over Surface I but there is also a considerable increase in reactivity. In the v=0 level if all the complexes were reactive the specific rate constant would be some three (at 2500°K) or four (at 1600°K) times larger than the minimum rate. Assuming here that the CLASTR integrator decision is correct for the complex trajectories, then the v=0 specific rate constant is only some 20 percent low at 2500°K and 30% low at 1600°K. In conclusion, it can be said in view of the above results for the specific rate constants that the total minimum constant rate would be in the worst case a factor of three too low due to the complexes. It seems much more likely to be low by some 20 to 30%. It would be nice to eliminate the complex problem altogether with an improved integrator for the trajectories. Since the last paper (Paper I) several variable step integrators[15,17] have been tried with no improvement over the CLASTR integrator.

As noted above the reactivity of at least some of the complexes causes the total rate constants calculated in Section III to be low. Also these rates will probably be low because of the greater reactivity of higher rotational states. As noted in Section III the higher rotational levels (data for J=21 level) are more reactive than the lower levels (data for J=1 level) perhaps by a factor of two. More trajectories should be run at various rotational levels to see if this tendency to greater reactivity is real or just due to statistical error.

Also the contribution of higher vibrational levels above v=6 should be investigated particularly at 2500°K. However, including these high vibrational levels ($v > 6$) means that some method for including the $H + O_2(^1\Delta_g)$ reaction would also have to be devised.

While it appears that the total rate constants calculated from trajectories for Surface II will be higher than experiment, the rate constant from the data for Surfaces I and I′ will be low. Total rate constants estimated for Surfaces I and I′ are some 25% of the experimental rates (at 1600°K and 2500°K) if the complexes are neglected. If it is assumed that the CLASTR integrator gives at least a statistically correct decision then these rates will be 50% of experiment.

As more accurate potential surface data become available for this reaction it should be possible to further refine the modified LEPS surface. Better dynamics calculations should then be possible.

---

15. J.L. Gole and E.F. Hayes, J. Chem. Phys., 57, 360 (1972).
16. W.H. Miller and T.F. George, J. Chem. Phys., 56, 5668 (1972). (Integrator described herein supplied by T. George.)
17. R. Van Wyk, J. of Computational Phys., 5, 244 (1970).

ACKNOWLEDGEMENTS

The author would like to thank Dr. Thomas O'Brien for reviewing some of the calculations of the potential surface derivatives. The author appreciates also the suggestions of Dr. George F. Adams.

REFERENCES

1. JANAF Tables, edited by D.R. Stull (Dow Chemical, Midland, MI, 1965-1967).

2. M.B. Collset, D.W. Naegeli, and I. Glassman, Sixteenth Symposium on Combustion (Combustion Institute, Pittsburgh, 1977) p. 1023.

3. T. Miyauchi, Y. Mori, and A. Imamura, Sixteenth Symposium on Combustion, (Combustion Institute, Pittsburgh, 1977) p.1073.

4. G. Dixon-Lewis and R.J. Simpson, Sixteenth Symposium on Combustion, (Combustion Institute, Pittsburgh, 1977) p. 1111.

5. A. Gauss, Jr., J. Chem. Phys. 68, 1689 (1978).

6. CLASTR is program No. 229 in the Quantum Chemistry Program Exchange Catalogue (QCPE, Indiana University, Chemistry Department).

7. D.S. Perry, J.C. Polanyi and C. Woodrow Wilson, Jr., Chem. Phys. 3, 317 (1974).

8. R.N. Porter, L.B. Sims, D.L. Thompson, and L.M. Raff, J. Chem. Phys. 58, 2855 (1973).

9. N. Sathyamurthy, J.W. Duff, C. Stroud, and L.M. Raff, J. Chem. Phys. 67, 3563 (1977).

10. N. Sathyamurthy, R. Rangarajan, and L.M. Raff, J. Chem. Phys. 64, 4606 (1976).

11. G.L. Schott, Combustion and Flame, 21, 357 (1973).

12. J.T. Muckerman, J. Chem. Phys. 56, 2997 (1972).

13. J.F. Ogilvie, Canadian Journal of Spectroscopy, 19, 171 (1973).

14. S. Farantos, E.C. Leisegang, J.N. Murrell, K. Sorbie, J.J.C. Texeira-Dias, and A.J.C, Varandas, Molecular Physics, 34, 947 (1977).

15. J.L. Gole and E.F. Hayes, J. Chem. Phys., 57, 360 (1972).

16. W.H. Miller and T.F. George, J. Chem. Phys., 56, 5668 (1972). (Integrator described herein supplied by T. George.)

17. R. Van Wyk, J. of Computational Phys., 5, 244 (1970).

DISTRIBUTION LIST

No. of Copies	Organization
12	Commander Defense Documentation Center ATTN: DDC-DDA Cameron Station Alexandria, VA 22314
1	Commander US Army Materiel Development and Readiness Command ATTN: DRCDMD-ST 5001 Eisenhower Avenue Alexandria, VA 22333
1	Commander US Army Aviation Research and Development Command ATTN: DRSAV-E P. O. Box 209 St. Louis, MO 63166
1	Director US Army Air Mobility Research and Development Laboratory Ames Research Center Moffett Field, CA 94035
1	Commander US Army Electronics Research and Development Command Technical Support Activity ATTN: DELSD-L Fort Monmouth, NJ 07703
1	Commander US Army Communications Rsch and Development Command ATTN: DRDCO-PPA-SA Fort Monmouth, NJ 07703
2	Commander US Army Missile Research and Development Command ATTN: DRDMI-R DRDMI-YDL Redstone Arsenal, AL 35809
1	Commander US Army Tank Automotive Rsch and Development Command ATTN: DRDTA-UL Warren, MI 48090
2	Commander US Army Armament Research and Development Command ATTN: DRDAR-TSS Dover, NJ 07801
1	Commander US Army Armament Materiel Readiness Command ATTN: DRSAR-LEP-L, Tech Lib Rock Island, IL 61299
1	Director US Army TRADOC Systems Analysis Activity ATTN: ATAA-SL, Tech Lib White Sands Missile Range NM 88002
1	Physical Sciences, Inc. ATTN: Dr. Alan Gelb 30 Commerce Way Woburn, MA 01801
1	Brookhaven National Laboratory ATTN: Dr. James T. Muckerman Upton, NY 11973
1	Texas Tech University Department of Chemistry ATTN: Dr. Thomas O'Brien Lubbock, TX 79409
	Aberdeen Proving Ground Dir, USAMSAA ATTN: Dr. J. Sperrazza DRXSY-MP, H. Cohen Cdr, USATECOM, ATTN: DRSTE-SG-H Dir, Wpns Sys Concepts Team, Bldg. E3516, EA ATTN: DRDAR-ACW